Role of frustration interactions in the thermal properties of tiling models for glasses

J. G. Harris and F. H. Stillinger
AT&T Bell Laboratories, Murray Hill, New Jersey 07974
(Received 10 July 1989)

To represent the apparent inability of supercooled liquids to form infinite amorphous well-bonded regions, we add frustration interactions to the Stillinger-Weber tiling model. Using a simple approximation to the tiling model entropy, we demonstrate that these frustration interactions, which limit tile sizes, can reduce a first-order phase transition to a continuous "transition" with a sharply peaked heat capacity. The role of frustration is explained using arguments similar to those that apply to finite-size effects in first-order phase transitions. When corrections from the virial series are added to the simple approximation to the tiling model entropy, previously unexpected first-order phase transitions appear even when limited frustration is present. Because such phase transitions are due to the constraints on the packings of hard cubes, they are artifacts of the tiling models' restriction to cubic domains and may not reflect the behavior of real glass formers.

I. INTRODUCTION

Glasses and deeply supercooled liquids represent states of matter that are far from equilibrium. The frequent dependence of the observable properties of the glass on factors such as the history of its preparation make it difficult to define good thermodynamic variables upon which to build a theory.

Glass-forming materials can be classified between "strong" and "fragile" extremes.[1,2] In the former, the dynamical properties, such as viscosity and self-diffusion, follow an Arrhenius type of behavior in which atoms presumably must cross a single type of activation barrier in order for the substance to flow.

In the fragile glass formers, the shear viscosity follows a strongly non-Arrhenius behavior, as if the activation energy increased with temperature decrease. Experimental evidence on some substances suggests that the product of the diffusivity and the viscosity can be much higher than that predicted by the Stokes-Einstein condition.[3,4] This indicates that shear flow involves the cooperative motions of many atoms, a process that should be slower than the self-diffusion of individual atoms.[5]

The supercooled liquids that form fragile glasses also exhibit an anomalously large heat capacity, i.e., much larger than the heat capacity of the solid phase.[6,7] The heat capacity continues to increase with decreasing temperature until the metastable liquid is cooled to the point at which the relaxation processes are too slow to permit equilibration on an experimental time scale. If the heat capacity at temperatures above this "glass transition" are used to extrapolate the entropy of the glass to lower temperatures, the extrapolation predicts that at some positive temperature, T_K, the Kauzmann point, the entropy of the glass will equal that of the crystal.[8] The suggestion that a second-order phase transition intercedes to prevent the entropy of the glass from dropping below that of the crystal has been discounted for substances with finite-range interactions.[9]

The theory of glasses suffers from the difficulty that the partition function of the substance is really dominated by the inaccessible (on the laboratory time scale) crystalline configurations. One solution to this problem is the use of the inherent structure formalism of Stillinger and Weber,[10] in which the partition function of N atoms interacting through a potential energy surface $U(\mathbf{r})$ is broken up into a sum of Boltzmann factors integrated around local potential energy minima,

$$Z=\frac{1}{N!}\sum_i \int_{\Omega_i} \exp[-U(\mathbf{r})/k_B T] d^{3N}r \ , \tag{1}$$

in which the region of the integration, Ω_i, around each minimum is the configuration space region which would collapse to the local minimum under a mass-weighted steepest-descent evolution. The amorphous-state partition function is defined by evaluating the sum over only basins which are noncrystalline, and the thermodynamic properties computed from this partition function are those of the supercooled liquid. These may differ from those observed in a laboratory experiment if sluggish relaxation does not permit the system adequately to sample the basins dominating the amorphous-state partition function.

The experimental evidence already presented suggests that in the supercooled fragile glass former, the atoms are clustered into well packed and strongly cohering amorphous (or even quasicrystalline) domains. The atoms at the edge of a domain experience weaker interactions than those in the interior, and the material can therefore flow by domains sliding against each other or forming new domain walls.[5] This accounts for the anomalously large viscosity of the deeply supercooled liquid. The "condensation" of atoms into larger domains as the substance is cooled should cause a large decrease in the internal energy, explaining the large heat capacity.

Stillinger and Weber developed a tiling model to study the qualitative nature of the distribution of domain sizes as a function of temperature in fragile glass formers.[11] To make the statistics more manageable, the tiling model is formulated on a d-dimensional cubic lattice with periodic boundary conditions, and all domains are cubic tiles with lengths that are integer multiples of the lattice

constant. Since the tiles represent the well-coordinated domains of the material, they must fill the lattice without overlapping and without leaving gaps. For the two-dimensional version, Monte Carlo simulations of Stillinger, Weber, and Frederickson,[12,13] and transfer-matrix calculations of Bhattacharee and Helfand[14] have provided accurate estimates of the thermodynamic properties. The entropy favors states with smaller domains, while the energy, which increases with the amount of boundary between domains, favors the formation of one macroscopic amorphous strongly bonded region. In a previous paper,[15] hereafter referred to as I, it has been shown that a first-order phase transition separates two states. It has also been shown that when frustration effects are present the first-order phase transition is replaced by rapid but continuous property variations.

The obstacle to the exact solution of the tiling model is the determination of the entropy as a function of the number of tiles of various sizes. In I, we presented an approximation to the entropy which is exact for a one-dimensional version of the tiling model. We demonstrated that when the ground state of the system is a macroscopic tile, this model predicts a first-order phase transition from a heterogeneous tiling, which we call the "liquid state," to a large macroscopic tile we refer to as the "condensed state." This phase transition is associated with a weak essential singularity in the free energy at which all derivatives approach finite values as the temperature approaches the transition from above. We also demonstrated that when the amorphous well-bonded domains are frustrated so that the formation of the macroscopic tile is prevented, this first-order phase transition disappears and is replaced by a continuous transition from a fine to a coarse tiling in a temperature range in which the heat capacity has a maximum. As the frustration energy becomes smaller and the ground-state tiles become larger, the maximum in the heat capacity becomes sharper.

In this paper we derive some systematic corrections to the tiling model entropy which significantly change its behavior when frustration is present. In particular the improved entropy, which incorporates the geometry of the tiles through a second virial coefficient approximation level, predicts the existence of new phase transitions when there is a limited amount of frustration. We also clarify the role of frustration and spatial dimensionality in the thermodynamics of the fragile glass formers near the glass transition.

The paper is divided as follows. In Sec. II, we briefly describe the tiling model and discuss the phase transitions predicted by it. In Sec. III we discuss the properties of the tiling model entropy function. We also develop two approximations to this entropy. In Sec. IV, we present the results of computations of the thermodynamic properties of the tiling model based on the two entropy approximations presented in III. In Sec. V we discuss a simple two-state model for incorporating the effects of frustrations which prevent the formation of macroscopic well-bonded domains. We compare the predictions of this conceptual model with those of the calculations presented in Sec. IV. In Sec. VI we summarize the implications of our model for the properties of real glass forming materials.

II. THE FORMULATION OF THE TILING MODEL

In the tiling model the medium is treated as a d-dimensional simple cubic lattice, completely covered by nonoverlapping tiles. To make the statistics of the system more manageable, we make the approximation that all tiles are cubic, (i.e., squares in the two-dimensional case) with lengths that are integer multiples of the lattice constant. Except for the excluded volume condition, there are no interactions between tiles. Hence in an allowed configuration of a system with n_l tiles of length l the internal energy is the sum of the energies of all the tiles,

$$E=\sum_{l=1}^{\infty} n_l \varepsilon_l \ , \tag{2}$$

where ε_l is the internal energy of each length l tile, and is assumed to be the same for all tiles of a given length, l. The fact that the tiles completely cover the lattice without overlapping implies that

$$\sum_{l=1}^{\infty} n_l l^d = V \ , \tag{3}$$

where V is the volume of the lattice in lattice spacing units.

The thermodynamics of the system is determined by the ε_l's and the number of distinct ways of arranging the tiles on the lattice. The energy of a length l tile can be divided into three contributions. First there is a bulk contribution, proportional to l^d, which does not affect the distribution of tiles because of the constraint in Eq. (2) and can thus be set to zero. The second contribution results from the fact that the atoms situated at a boundary between tiles have a less favorable potential energy compared to interior atoms. The number of these atoms and hence the energy should be proportional to the boundary size, l^{d-1}. The third contribution occurs when the well-bonded amorphous packings do not completely fill space in the Euclidean dimension of the system. If the amorphous packings are natural in some dimension d',[16] then as shown in Appendix A, there should be an energy penalty proportional to $l^{d+\nu}$, where $\nu=|d-d'|$. Thus the tile energies should be

$$\varepsilon_l = d(\lambda l^{d-1}+\theta l^{d+\nu}) \ . \tag{4}$$

In this work, λ will always be assumed to be 1. A rescaling of temperature and θ will generalize this to all values of λ.

In an experiment, the number of particles, the temperature, and either the pressure or volume of the system can be maintained at particular values. The texture of the material, i.e., the distribution of domain sizes, remains uncontrolled. Thus the material should adopt the texture which minimizes the free energy. In the tiling model, this means adopting the concentrations of tile sizes, $\rho_l = n_l/V$, which minimize the free-energy density function,

$$f[\{\rho_l\}]=e[\{\rho_l\}]-T\sigma[\{\rho_l\}] , \tag{5}$$

where the energy density is e and the entropy density is σ. The temperature, T, is in units such that $k_B=1$. In the infinite system limit, the number of distinct ways of arranging the $\{n_l\}$ tiles in an allowed configuration is $\exp(V\sigma)$. When $\theta=0$ the system exhibits a first-order phase transition between the macroscopic tile ($l\approx V^{(1/d)}$) of the condensed state and a heterogeneous tiling of the liquid state. At the condensation point of the $\theta=0$ system, the minimum free energy is zero. At higher temperatures, the entropy effect dominates and the free energy is negative. At any lower temperature the macroscopic tile has a lower free energy than any other distribution of tile sizes.

III. THE TILING MODEL ENTROPY

To evaluate the temperature of condensation, the heat of condensation, and other thermodynamic properties, it is necessary to compute the entropy of a given distribution of tiles. Currently, it is impossible to compute an exact entropy; however, it is possible to deduce several properties of the entropy function from the geometry of the tiling model and thus to develop some reasonable approximations for σ. In this section we will summarize the known properties of σ, and then present a derivation for an approximation to σ similar in spirit to the scaled particle theory of hard spheres.[17]

The five conditions that the entropy should satisfy are (i) a scaling law, (ii) the existence of a viral expansion in the limit that $\rho_l\to 0$ for all $l\geq 2$, (iii) the existence of a homogeneous form for the entropy, (iv) the "dense tiling limit"—a limiting behavior when the system is dominated by tiles of one size, $l>1$, and (v) a convexity condition.

The scaling law, presented in I, is

$$\sigma[\{\rho_l\}]=b^d\sigma[\{\rho_l^{(b)}\}], \tag{6}$$

where b is a positive integer, $\rho_{bl}^{(b)}=b^{-d}\rho_l$, and $\rho_l^{(b)}=0$ whenever l is not a multiple of b. This condition is justified by the fact that if all of the tile lengths are increased by a factor of b and the system volume is also increased by a factor of b^d, the number of ways of arranging the tiles is unchanged, aside from a translation factor (with periodic boundary conditions) which does not increase exponentially with system size and thus cannot affect the thermodynamics. The scaling condition trivially implies that the entropy density of a tiling with only one tile size must be zero, because a function that follows the scaling law and is zero for the uniform system of the unit size tiles will be zero for all uniform tilings.

A virial expansion can be derived by considering the uniform system of length 1 tiles as the empty system, i.e., a "vacuum." The entropy of a partially filled system with no length 1 tiles and a distribution, $\{\rho_l\}$, remains unchanged when all of the vacancies are replaced by length 1 tiles. In the noninteracting limit the entropy is

$$\sum_{l\geq 2}\rho_l[1-\ln(\rho_l)] . \tag{7}$$

Corrections for the excluded volume can be computed from the irreducible cluster diagrams. Because the excluded volume interaction is repulsive, the next two virial corrections are negative. The second-order correction to Eq. (7) is

$$-\tfrac{1}{2}\sum_{k,l\geq 2}(k+l-1)^d\rho_k\rho_l . \tag{8}$$

Higher-order corrections quickly become very complicated and computationally intractable.

The third condition observes that the entropy can be written as a homogeneous function of the ρ_l's ($l\geq 1$),

$$\mu_0 g[\{\rho_l/\mu_0\}] , \tag{9}$$

where the moments are defined as

$$\mu_p=\sum_{k\geq l}\rho_k k^p . \tag{10}$$

Because the entropy is defined only at complete filling, there may be many physically equivalent ways of writing σ as a function of all of the tile concentrations. In Appendix B, we show that the equilibrium tile concentrations for large k behave asymptotically as

$$\ln(\rho_k)\sim\beta f[\{\rho_l\}]k^d-\beta\varepsilon_k , \tag{11}$$

where $\beta=1/(k_BT)$. The minimization of the free energy subject to the constraint in Eq. (2) implies

$$\beta\varepsilon_l-\frac{\delta\sigma}{\delta\rho_l}=\Lambda_d l^d , \tag{12}$$

where Λ_d is the Lagrange multiplier. The derivative of the entropy includes a $\ln(\rho_l)$ term so that the solution to Eq. (12) is

$$\ln(\rho_l)=\Lambda_d l^d-\beta\varepsilon_l+(\text{terms from the entropy derivative}) . \tag{13}$$

The terms from the entropy derivative may contain at most contributions proportional to l^d which can be removed by redefining the entropy function, as is allowed because any function of the ρ_k''s which is also zero when the constraint in Eq. (3) is met can be added to σ. The resulting function will still be the entropy for any physically relevant tiling. There is a unique σ which produces no l^d terms in the parentheses of Eq. (13) and is the entropy of the tiling at complete filling. In such a case, Eqs. (11) and (13) require $\Lambda_d=\beta f$.

To prove the homogeneity condition, we then multiply Eq. (12) by ρ_l and sum over all l to obtain

$$\sigma[\{\rho_l\}]=\sum_{l\geq l}\rho_l\frac{\delta\sigma}{\delta\rho_l} . \tag{14}$$

This is equivalent to the stated homogeneity condition, which only holds for the equilibrium concentrations of the tiles. Except in the vicinity of a singularity in the entropy, the equilibrium concentrations can be continuously varied by changing the tile energies.

The fourth condition states that when a binary system of length k and length l tiles approaches the limit of a uniform tiling of length l tiles, the entropy should approach zero as

$$[k/(k,l)]^{(d-1)}\rho_k\ln(\rho_k) , \tag{15}$$

where (k,l) is the least common multiple of k and l. In this limit most of the size k tiles are geometrically forced to appear in aggregates of size $[(k,l)/k]^{(d-1)}$. The aggregation is most easily seen in a mixture of 2×2 and 1×1 tiles in the square tiling model ($d=2$), illustrated in Fig. 1. In order to place four 1×1 tiles on the lattice when the other tiles are 2×2, the four tiles must be in the form of two aggregates of two tiles each. In order to fit an isolated 1×1 tile into the matrix, a total of at least twelve 1×1 tiles must be inserted, as shown, for example, in Fig. 1(b)—two of these in a fixed configuration and several of the rest subject to constraints in their positions. Hence in a dilute solution of 1×1 in a matrix of 2×2, the dimers will predominate, as more configurations can be generated from a group of dimers than from a cluster producing isolated 1×1 tiles. Equation (15) for this example is the dilute limit for the entropy of mixing of the binary aggregates. A similar argument for a general pair of sizes, k and l, leads to the common form of Eq. (15).

The fifth condition requires that $-\sigma$ be a convex function of the densities. If there are two macroscopic systems of volumes V and V' and respective tile distributions $\{\rho_l\}$ and $\{\rho'_l\}$, the combined entropy of the systems is just the sum of the entropies. If the two systems are combined and their tiles are no longer kept separated, a new system is formed with volume $V+V'$ and tile concentrations $\alpha\rho_l+(1-\alpha)\rho'_l$, where $\alpha=V/(V+V')$. Its entropy must be no less than that of the two separate systems because the combined system is no longer subject to the constraint that the two subsystems have the tile concentrations $\{\rho_l\}$ and $\{\rho'_l\}$. Thus

$$\sigma[\{\alpha\rho_j+(1-\alpha)\rho'_j\}]\geq\alpha\sigma[\{\rho_j\}]+(1-\alpha)\sigma[\{\rho'_j\}]\ . \quad (16)$$

Whenever the internal energy is of the form of Eq. (2), the free energy is also convex.

In the following discussion we derive an approximation to the tiling model entropy based on the scaled-particle theory of hard spheres. This approximation was presented without derivation in I. We first note that the entropy of a distribution of tiles all of lengths greater than or equal to 2 which do not completely fill the lattice is unchanged by the placement of 1×1 tiles on all of the empty lattice spaces. Thus we can remove from consideration the 1×1 tiles and the complete filling constraint [Eq. (3)]. The entropy and its partial derivatives with respect to ρ_k are thus well-defined functions of the ρ_k, where $k\geq2$. When k is large, the entropy change that occurs when a size k tile is added to the system can be broken up into a translational term representing the change in the translational entropy of the size k tiles, a "bulk" term proportional to the volume of the inserted tile, resulting from the fact that when the location of the added tile is fixed the volume available to the other tiles is reduced by k^d, and a geometric term proportional to the size of the inserted boundary, resulting from the geometric constraints imposed by the insertion of the size k tile. As shown in Appendix B, this scaled particle theory predicts

$$\frac{\delta\sigma}{\delta\rho_k}=-\ln(\rho_k)+\ln(1-\mu'_d)-(k^d-1)\sigma[\{\rho_l\}]+(k^d-1)\sum_{l\geq2}\rho_l\left[\frac{\delta\sigma}{\delta\rho_l}\right]+b_k[\{\rho_l\}]\ , \quad (17)$$

where b_k is the "geometric term" of order k^{d-1}, and the primed moments of the tile size distribution are

$$\mu'_p=\sum_{k\geq2}k^p\rho_k\ . \quad (18)$$

It is important to note that solutions to Eq. (17) do not exist for arbitrary functions $b_k[\{\rho_j\}]$. When $b_k=0$ the solution to Eq. (17) is

$$\sigma_0=-\sum_{k\geq l}\rho_k\ln(\rho_k/\mu_0)\ . \quad (19)$$

This entropy is consistent with the virial expansion to first order and follows all of the other conditions, except for (iv), the "high-density-limit condition." We refer to σ_0 as the "one-dimensional approximation" to the entropy, because it is the exact entropy of a set of $\{n_l\}$ rods with lengths l^d on a line of length V.

Two routes are available to improving our estimate of σ. One is the development of approximations for b_k; and

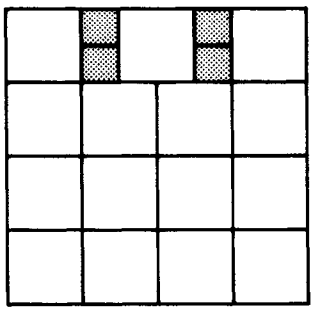

(a)

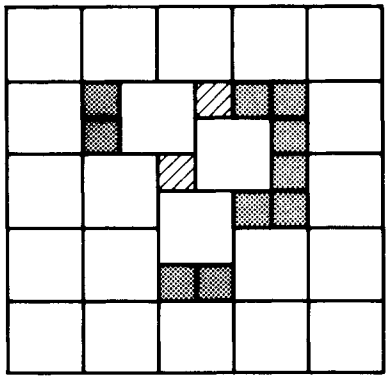

(b)

FIG. 1. Allowed arrangements of 1×1 tiles in a matrix of 2×2 tiles. (a) Dimerized 1×1 tiles. (b) The configuration with the fewest number of 1×1 tiles in which some 1×1 are not dimerized. The hatched squares cannot move relative to each other.

the other is the addition of terms to σ_0 which maintain its scaling property and its homogeneity and make it consistent with the virial expansion to a given order. We have not been able to develop approximations of this latter kind for b_k for which Eq. (17) has a solution. However, the second procedure has been carried out to produce an approximation to σ that is consistent with a second-order virial expansion and all of the other conditions except for convexity and the high-density-limit condition. Note that this procedure does not uniquely define σ.

The simplest approximation to σ consistent with the virial expression to second order and satisfying the scaling and homogeneity conditions is

$$\sigma_2[\{\rho_l\}]=\sigma_0[\{\rho_l\}]-\frac{1}{2\mu_0^2}\sum_{k\geq 1}\sum_{l,m\geq 2}[(kl+km-1)^d-(kl)^d-(km)^d+1]\rho_k\rho_{kl}\rho_{km} \ . \tag{20}$$

IV. CALCULATIONS

The equilibrium distributions of tiles for many values of β, θ, and ν and $d=2$ and $d=3$ have been determined by solving Eq. (12) by simple iteration using the entropy approximations of Eqs. (19) and (20). The sums are truncated at a value of $l=N_C$. This is equivalent to a tiling model with a maximum allowed tile size. When $\theta=0$ a value of $N_C=100$ is adequate to obtain acurate results, although there is a very slight rounding of the liquid-condensed phase transition. At each step in the iteration the right-hand side of Eq. (13) is calculated using an estimate for the density obtained from the previous iteration and the Lagrange multiplier chosen so that the constraint in Eq. (3) is satisfied. (In some cases using entropy approximation σ_2, the input and output tile concentrations must be mixed to obtain efficient convergence of the iterations.) Λ_d is found by using the bisection method followed by Newton's method. The procedure is continued until the change in the absolute value of the densities is less than one part in 10^{11}. In generating tile concentrations as a function of β for a sequence of β's the initial tile concentrations supplied to the iterative procedure are equilibrium concentrations at the previous value of β.

When the one-dimensional entropy approximation, σ_0, is used the procedure can be simplified to just finding the Lagrange multiplier satisfying

$$\sum_{l=1}^{l=N_c}\exp[\Lambda_d l^d-d\beta(l^{d-1}+\theta l^{d+\nu})]=1 \tag{21}$$

using a bisection method followed by Newton's method. In this case the tile densities are given by

$$\rho_k=\frac{\exp[\Lambda_d k^d-d\beta(k^{d-1}+\theta k^{d+\nu})]}{\sum_{l=1}^{l=N_C} l^d\exp[\Lambda_d l^d-d\beta(l^{d-1}+\theta l^{d+\nu})]} \ . \tag{22}$$

When $\theta=0$ both entropy approximations predict a first-order phase transition between a heterogeneous tiling and a large macroscopic tile. This condensation occurs at β_c, the value of β at which $\Lambda=\beta f=0$. The condensation point and latent heats of the transitions in two and three dimensions are shown in Table I along with the values predicted by the transfer matrix, computer simulations, and an earlier mean-field theory.[10]

In Figs. 2 and 3 we compare the entropy, energy, and free energies as functions of temperature according to entropy approximations σ_0 and σ_2. The virial correction significantly improves the location of the condensation point and the latent heat because small tiles predominate at the transition. However, it violates the convexity condition at high concentrations of larger tiles. In particular, the entropy of a binary mixture of 1^d tiles and l^d tiles is not concave (i.e., $-\sigma_2$ is not convex) near complete coverage with l^d tiles when $d=2$ and $l\geq 3$ and when $d=3$ and $l\geq 2$ as demonstrated in Fig. 4. A free energy satisfying the convexity property can be constructed from σ_2 using the double tangent rule. When the maximum allowed tile size (N_C) is finite, two local free energy minima occur in $\{\rho_l\}$ space. Because the initial guess used to start the iterative procedure to find the equilibrium tile concentrations at β is the equilibrium distribution of tiles at an adjacent β on the curve, two separate curves of tile distributions versus β are obtained. They correspond to starting in the vicinity of one or the other minimum. Of course the correct distributions are those corresponding to the lowest free energy, and the liquid-condensed transition of the finite system in which $N_C=\infty$ occurs at the point where the free energy of the correct distribution becomes zero.

The presence of frustration, $\theta\neq 0$, causes the singularity in the free energy to disappear completely from the one-dimensional appoximation. Instead the heat capacity shows a maximum, which broadens as θ increases. The

TABLE I. The tiling model phase transition: location and heats of condensation.

	$d=2$		$d=3$	
Source	β_c[a]	Δe[b]	β_c	Δe
Monte Carlo/Padé[c]	0.271	0.943		
Transfer matrix[d]	0.270			
Mean field[e]	0.628			
Using σ_0[f]	0.347	0.667	0.116	1.57
Using σ_2[f]	0.264	1.008	0.073	2.12

[a] β_c is the condensation point at which $f=0$.
[b] Δe is the latent heat of the transition.
[c] Obtained by fitting a Padé approximate to Monte Carlo simulations and the energy expansion around $\beta=-\infty$. See Refs. 12 and 13.
[d] See Ref. 14.
[e] See Ref. 11.
[f] From this work.

ground state is no longer a macroscopic tile, but a uniform tiling of size $l \approx (\nu\theta)^{-1/(\nu+1)}$, except at discrete values of θ in which there are two tile sizes with equal energy densities lower than those of any other tile. Accurate numerical distributions of tiles can be obtained as long as N_C, the maximum tile size appearing in the summations, is at least one and a half times the ground-state tile size. In Fig. 5 we show heat capacity as a function of β for several values of the frustration exponents for both two and three dimensions.

Under entropy approximation σ_2, frustration removes the liquid-condensed phase transition; but the nonconvexity of the approximate free energy induces another kind of first-order transition. All calculations done with this approximation for the entropy used the frustration exponent $\nu = 1$. The two phases differ in that the one

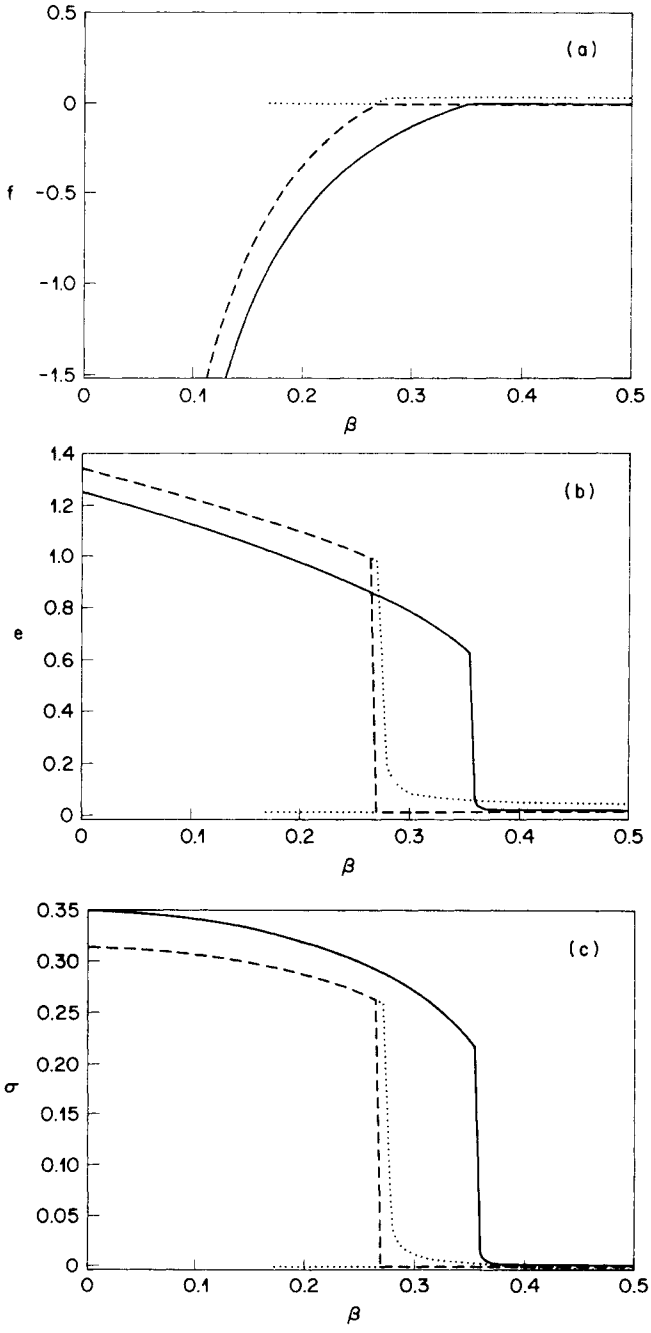

FIG. 2. Thermodynamic functions of the equilibrium tiling of the $d = 2$ tiling model computed using entropy approximations σ_0 (solid line) and σ_2 (dashed line), and the extra solution of the model using σ_2 (. . .) (when $N_C = 100$) (a) free energy density, (b) internal energy density, and (c) entropy density.

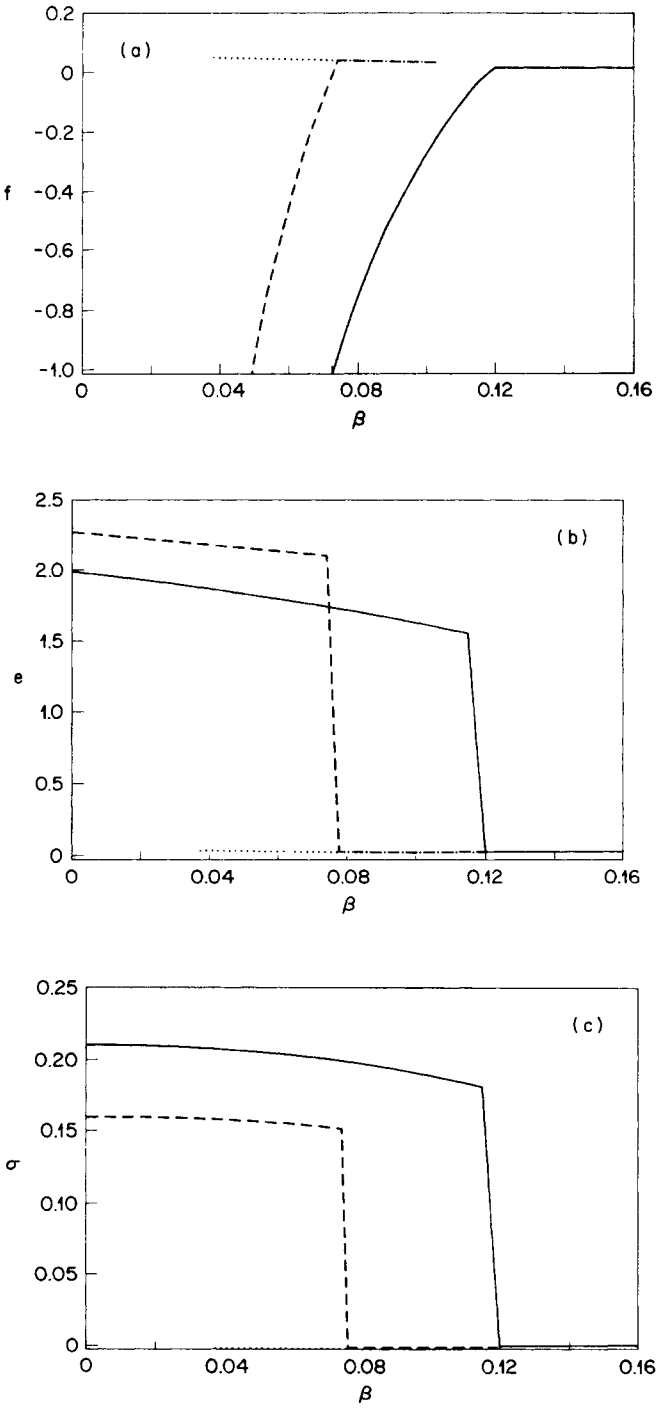

FIG. 3. Same as Fig. 2, but for the three-dimensional tiling model.

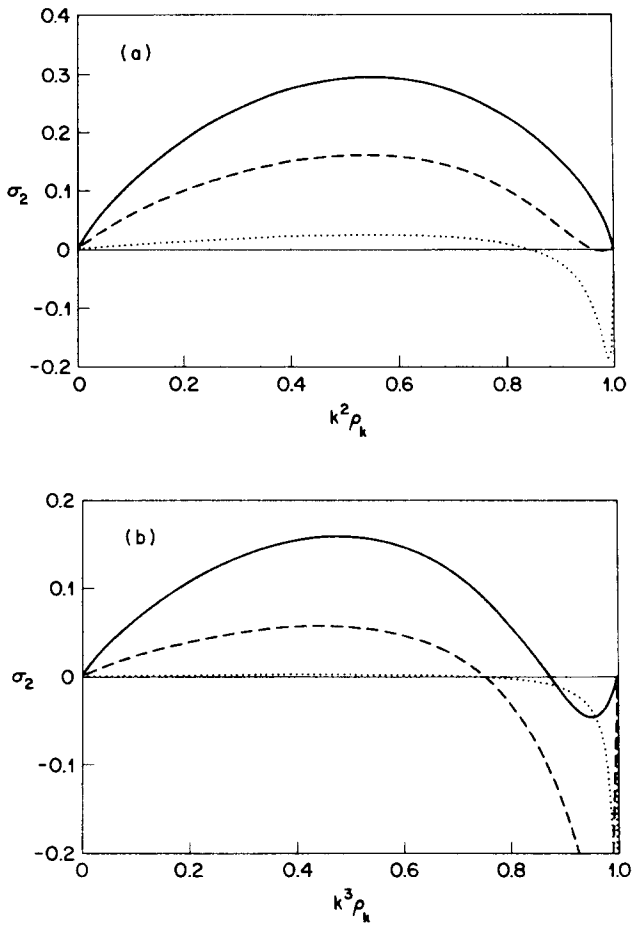

FIG. 4. σ_2 of binary mixtures of unit size and length k tiles for the (a) two-dimensional and (b) three-dimensional tiling models. The lines correspond to $k=2$ (solid line), $k=3$ (dashed line), and $k=10$ (dotted line).

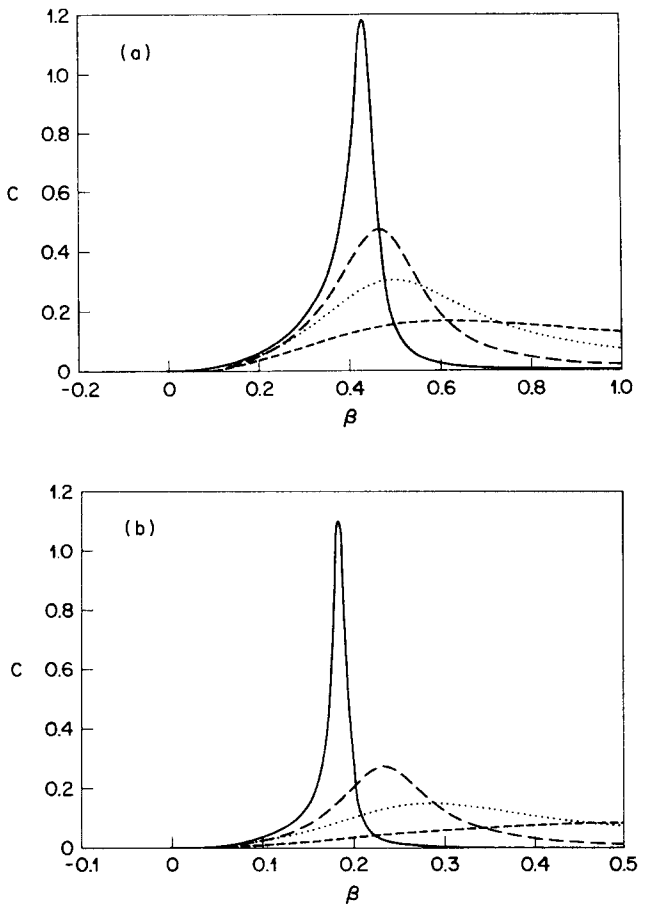

FIG. 5. Heat capacity of the frustrated tiling model using entropy approximation σ_0 with frustration exponents of 0.5 (solid line), 0.75 (solid-solid line), 1.0 (dotted line), and 1.5 (dashed line). (a) Two dimensional tiles with $\theta=0.01$. (b) Three-dimensional tiles with $\theta=0.05$.

stable at low temperature lacks the unit size tiles, while the one stable at high temperature has a significant concentration of these tiles. In Fig. 6, we compare the concentrations of tiles that appear in these two phases at the transition point for this system. In two dimensions, this transition has a critical point at $\theta_c=0.117$ and $\beta=0.84$, while in three dimensions the critical point is at $\theta_c=0.5$ and $\beta=\infty$. For $\theta>\theta_c$ no phase transition occurs. In the three-dimensional case this can be easily understood, because when θ exceeds 0.5, the ground state becomes the uniform tiling of unit size tiles and there is no driving force for the transition. In the two-dimensional case, because the entropy is convex for a mixture of 1×1 and 2×2 tiles there should be no phase transition for $\theta>\frac{1}{6}$, but the effects of the frustration prevent the free energy from having multiple minima at an even lower θ. As θ approaches θ_c the two phases become similar, hence the appearance of unit size tiles in the condensed phase in the $d=2$, $\theta=0.115$ case shown in Fig. 6(a).

V. SIMPLE MODEL DESCRIBING PHASE TRANSITION FRUSTRATION

The one-dimensional approximation, σ_0, predicts the disappearance of the phase transition under any positive amount of frustration. The disappearance of the phase transition with frustration can be understood using a two-state model similar to that described in Hill[18] and arguments similar to the finite-size-scaling theory.[19,20]

Nonzero values of θ introduce a natural length scale $L_C\approx(\theta\nu)^{-1/(1+\nu)}$, the ground-state tile size. (The ground-state tile size must be one of the two integers bracketing L_C.) Fluctuations to much larger tile sizes are forbidden because of the large frustration energy. We can thus divide the substance into regions of length L_C. In a real substance, it is reasonable to expect that the tiling of a region of size L_C does not strongly affect the tiling of adjacent regions. The heat capacity per unit volume is

$$C=\beta^2\left\langle\frac{(E-\bar{E})^2}{V}\right\rangle . \tag{23}$$

Near the transition temperature, the dominant fluctuations in the energy will be from the heterogeneous tiling to very large squares of size L_C. Neglecting the small energy of the condensed state, each region will experience a mean-square total energy fluctuation proportional to approximately $(e_L L_C{}^d)^2$, where e_L is the energy density of the liquid state. The mean-square total energy fluctuation of the entire system is the sum of the mean-square total energy fluctuations of all of the V/L_C^d regions and hence the heat capacity maximum is proportional to

$$C\approx\beta^2 e_L^2 L_C^d\approx\beta^2 e_L^2(\theta\nu)^{-d/(1+\nu)} . \tag{24}$$

A more quantitative argument proceeds by classifying the available states in each region as either liquid or condensed, the condensed state being one tile filling the whole region. The partition function for a region can be separated into a sum over all of the liquid states, the liquid partition function, and a sum over the condensed states, the condensed partition function. The total partition function of the material is

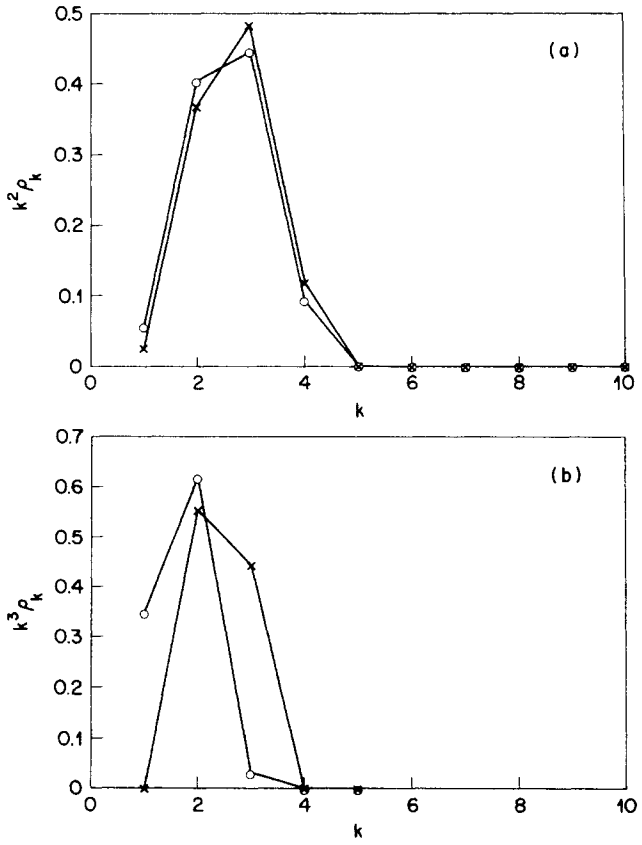

FIG. 6. Fraction of volume covered by length l squares, $l^d\rho_l$, as a function of l for the low-temperature phase (×) and the high-temperature phase (○) when entropy approximation σ_2 is used. (a) $d=2$, $\theta=0.115$, $\beta=0.83933$ (b) $d=3$, $\theta=0.20$, $\beta=0.34525$. In both cases β is approximately the transition point.

$$Z=(z_L+z_C)^{N_R} , \tag{25}$$

where $N_R=V/L_C^d$ is the number of regions and z_L and z_C are the liquid and condensed partition functions for a region, respectively. We can approximate Eq. (25) by the maximum term in its binomial expansion. The logarithm of this maximum term is the total free energy, thus the fraction of regions in the liquid state is

$$x_L=\frac{z_L}{z_L+z_C}=\frac{1}{1+\exp[-\beta(f_C-f_L)]} \tag{26}$$

and the free energy density is

$$\begin{aligned} f&=\frac{1}{\nu}[x_L\ln(x_L)+(1-x_L)\ln(1-x_L)] \\ &\quad+x_L(e_L-T\sigma_L)+(1-x_L)(e_C-T\sigma_C) \\ &=f_L-(1/\beta\nu)\ln\{1+\exp[\nu(-\beta\Delta e+\Delta\sigma)]\} , \end{aligned} \tag{27}$$

where f_L is the liquid free energy, $\nu=L_C^d\approx(\theta\nu)^{-d/(\nu+1)}$ is the region size, $\Delta e=e_C-e_L$, $\Delta\sigma=\sigma_C-\sigma_L$, and $\Delta f=\Delta e-T\Delta\sigma$. For any finite value of ν this function is analytic and varies smoothly from the liquid to the condensed free energy. When ν becomes infinite, a singularity appears at $\Delta f=0$ where the two free energies are equal and the slope is discontinuous.

The heat capacity is the second temperature derivative of Eq. (27) and is approximately

$$C\sim\frac{\beta^2\nu(\Delta\varepsilon)^2\exp(\beta\nu\Delta\varepsilon-\nu\Delta\sigma)}{[1+\exp(\beta\nu\Delta\varepsilon-\nu\Delta\sigma)]^2} , \tag{28}$$

where the derivatives of f_L, Δe, and $\Delta\sigma$ have been omitted because they are insignificant contributors to the heat capacity peak. The addition of these terms would make the heat capacity higher on the liquid side, since in this model the liquid phase has more excitations available. To estimate the position and height of the heat capacity peak, we make the approximation that $\Delta\sigma$ is the entropy of the transition of the unfrustrated model and $\Delta e\equiv\Delta e_0+\varepsilon_{L_c}-d\theta\mu_{\nu+d}^0$, where Δe_0 is the latent heat of the phase transition without frustration, and the other terms correct for the shift in the energy of the liquid and condensed phases due to frustration. $\mu_{\nu+d}^0$ is the moment [defined in Eq. (10)] of the unfrustrated system at the transition point. It is these corrections which produce the shift in the heat capacity maximum towards lower temperature.

The maximum in the heat capacity should occur at the temperature at which $\Delta f=0$, and should be $\beta^2\Delta e^2(\nu\theta)^{-d/(\nu+1)}$. Because the heat capacity maximum occurs at $\beta_M=\Delta\sigma/\Delta e$, the temperature shift is given by $\Delta\sigma/\Delta\varepsilon-\Delta\sigma/\Delta\varepsilon_0\to K\theta^{1/(\nu+1)}$ as $\theta\to0$ where K is a positive multiplicative constant. The width of the heat capacity curve is approximately the latent heat of the transition divided by the height of the curve. Two fair requirements of this approach are that it reproduces the scaling behavior of the one-dimensional approximation and that it reproduces the temperature shift. The former can be tested by plotting the logarithm of the heat capacity maximum as a function of the logarithm of L_C for various

values of f and d. As $L_C \to \infty$ the slope of the plot, shown in Fig. 7, approaches d for all of the three values of ν tested. In Fig. 8, we compare $\ln(\beta_M - \beta_C)$ with $\ln(L_C)$. The slope of the plot approaches $1/(\nu+1)$ as $\theta \to 0$.

It appears that this two-state approach gives a reasonable description of the development of the singularity in the free energy as the frustration vanishes. We note that even the one-dimensional rod model cannot be completely described as a set of regions of size L_C since there are certainly liquid regions much smaller than L_C which can be surrounded by condensed domains. This does not affect the scaling exponents in the low frustration limit. Its applicability to the square or cubic tiling model hinges on the assumption that there are no infinite-range correlations in the system. In the next section, it will be argued that such correlations are not relevant to the physics in real fragile glass-forming materials.

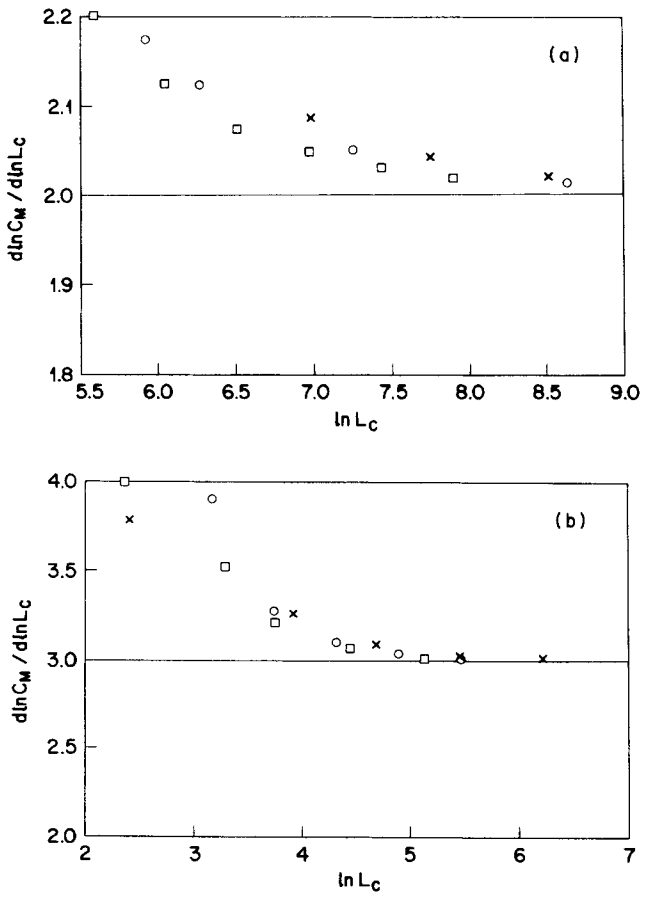

FIG. 7. The derivative $d\ln C_M / d\ln L_C$ where C_M is the maximum heat capacity as a function of the logarithm of L_c for (a) $d=2$ and (b) $d=3$. The frustration exponents are $\nu=0.5(\times)$, $\nu=1.0(\circ)$, and $\nu=1.5$ ($\square$).

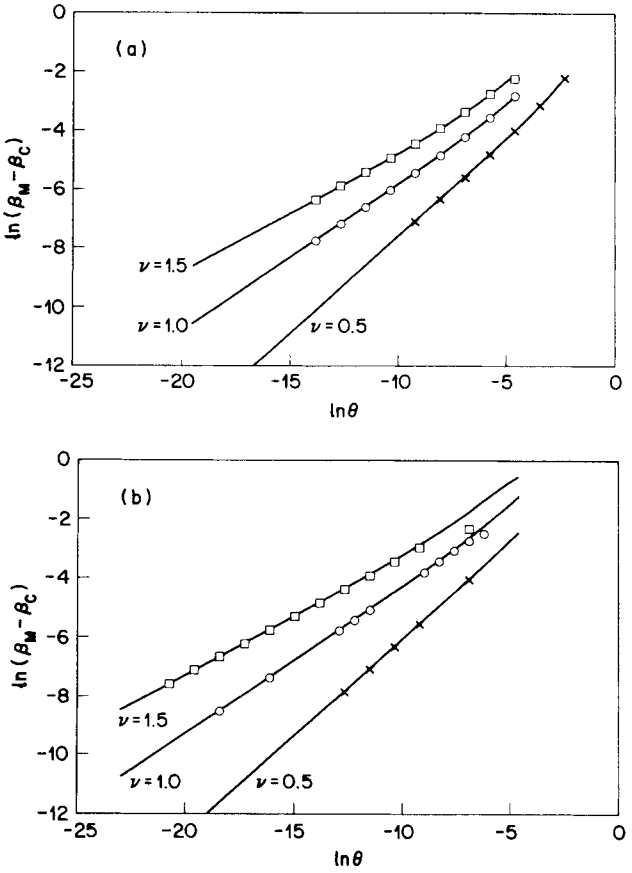

FIG. 8. The logarithm of $\beta_M - \beta_c$ as a function of θ for (a) $d=2$ and (b) $d=3$. The solid lines are predicted from the two-state model and the exponents shown are $\nu=0.5(\times)$, $\nu=1.0(\circ)$, and $\nu=1.5(\square)$. The symbols are the values of $\ln(\beta_M - \beta_c)$ predicted by the solution of the one-dimensional model.

VI. DISCUSSION

In this section we discuss the relevance of the calculations already presented to the exact square tiling model and to the real fragile glass-forming materials. The model for the frustration effects hinges on the assumption that there are no infinite-range correlations in the tile distribution which would correspond to singularities in the entropy as a function of the tile concentrations, as is suggested by the virial correction to the one-dimensional model. The methods used in this paper prevent the entropy approximations from exhibiting any such singularity; however, as in the mean-field theories, the free energy may become concave in the region around the singularity. Such phase transitions could preempt the continuous transition. At this time, we cannot make a conclusive statement on the existence of such phase transitions in the tiling models; however calculations on hard square lattice gases may shed some light on the issue.[21]

For example a binary mixture of 1×1 and 2×2 square

tiles is equivalent to the lattice gas with first- and second-neighbor exclusions. This particular two-dimensional lattice gas has been studied using virial series,[22,23] high-density expansions,[22] and transfer-matrix techniques.[22,24–26] The different authors have claimed that there are no phase transitions at densities less than close packing,[23] that there is a second-order phase transition,[22,25,26] and that there is a third-order phase transition.[24] All studies agree that there is no first-order phase transition. The application of finite-size scaling to the transfer matrices[25,26] indicates the existence of a second-order phase transition in the system at $\rho_2 \approx 0.24$. Other studies have demonstrated that the lattice gas with nearest-neighbor exclusions has a second-order phase transition, while the lattice gas with first-, second-, and third-nearest-neighbor exclusions has a first-order transition.[21] This pattern is consistent with the entropy approximation σ_2. As the excluded volume of the particle becomes isotropically larger, the tendency towards a first-order phase transition becomes greater, as the system becomes more like the hard disk fluid. We are aware of no studies done on the three-dimensional hard-core lattice gases, for which σ_2 predicts a first-order phase transition even for first-, second-, and third-neighbor exclusions (the mixture of $1\times1\times1$, and $2\times2\times2$ tiles). Although σ_2 implicitly includes corrections to the virial expansion of all orders, it would be premature to assume that our calculations describe the phases of the lattice gases accurately. We also note that the third-order irreducible diagrams are always negative, so that adding this correction will not qualitatively change the conclusions presented in this work.

The differences between the square tiling model and the one-dimensional approximation to it are substantially irrelevant to the statistical mechanics of the fragile glass formers. These differences arise from the packing restrictions imposed by the use of only square domains. In a real glass former, large domains would reduce the total entropy in proportion to their volume; but the domain shapes can be adjusted to allow the domains to fit together.

Frustration can occur when the shapes of the atoms or molecules prevent the amorphous well-bonded packings from compactly filling space. Phillips has suggested that a similar form of frustration can occur in amorphous covalent network glasses, i.e., Si and Ge.[27] In these substances, the number of constraints on each atom originating from the strong covalent bonds exceeds the number of degrees of freedom—the spatial dimension. In the crystal these constraints are redundant; but if the liquid is quenched too rapidly for the relaxation to a crystalline structure to occur, a highly strained covalent network is formed.

The calculations reported here show that in these two cases, the frustration energy limits the size of the domains that form and a singularity in the thermodynamic functions is completely avoided. As demonstrated in Secs. IV and V, the formation of large domains of well-packed atoms can account for an anomalously large heat capacity. It has also been argued that this domain formation also accounts for the rapid increase in the viscosity near the glass transition, which accompanies the large heat capacity.[5] If a material showing the behavior of the one-dimensional approximation to the tiling model were being studied in the laboratory, the maximum in the heat capacity peak would likely not be observed; when the temperature gets low enough to form the larger domains, the relaxation becomes so slow that heat capacity measurements depend on the history of the sample's preparation and the duration of the experiment. The observer extrapolates the heat capacity beyond the observed apparent maximum and thus obtains the Kauzmann point where the entropy of the glass would equal the entropy of the solid. As our calculations show, such extrapolation is risky and the Kauzmann paradox can be avoided without any phase transition. The avoidance of the first-order phase transition could occur in the formation of microcrystalline phases in cases for which the atoms of these materials cannot fill the space compactly in the crystal or quasicrystal packings. In cases where the crystal, quasicrystal, or amorphous packings of a group of atoms can fill the space, a first-order phase transition in principle appears abruptly at a temperature at which the excess entropy of the collection of small domains no longer compensates for the energy associated with the defects along the boundary.

APPENDIX A: FRUSTRATION ENERGY AND PACKING

In this appendix we propose a rationale for our form for the frustration energy. If a well-packed structure of the substance is "natural" in d' instead of d dimensions, then in a spherical shell of thickness δr at a distance r from some central particle the amount of substance should be proportional to $r^{d'-1}\delta r$. The frustration energy results when this shell is stretched or compressed to a surface of size r^{d-1}. If this compression or expansion is small enough for linear elasticity theory to apply and radial contraction or expansion effects are small, the shell contributes

$$\tfrac{1}{2}K\frac{(r^{d-1}-r^{d'-1})^2\delta r}{r^{d'-1}} \tag{A1}$$

to the frustration energy. Here K is a suitable elastic constant. The total frustration energy is just the integral of the shell contributions from the minimum particle size to the region radius, $R = l/2$, which is

$$K\left[\frac{R^{2d-d'}}{2d-d'}-\frac{2R^{d}}{d}+\frac{R^{d'}}{d'}\right]+C\ , \tag{A2}$$

where C is the constant of integration. For large tile sizes this frustration energy is dominated by the term with the largest exponent, $\nu+d = d+|d-d'|$.

APPENDIX B: THE DERIVATION OF EQ. (17) AND THE ASYMPTOTIC BEHAVIOR OF THE CONCENTRATIONS OF LARGE TILES

The derivative $\delta\sigma/\delta\rho_k$, where σ is treated as a well-defined function of $\{\rho_k\}$, for $k \geq 2$, is

$$\frac{\delta\sigma}{\delta\rho_k}=\ln\left[\frac{\Omega[\{n_l\},n_k+1,V]}{\Omega[\{n_l\}]}\right] . \tag{B1}$$

$\Omega[\{n_l\},V]$ is the microcanonical partition function, the number of ways of arranging the n_l tiles in a volume V on the lattice, and the notation "$[\{n_l\},n_k+1]$" means the system with $\{n_l\}$ tiles, but with 1 additional length k tile replacing k^d unit length tiles. We introduce the partition function, $\Omega_k[\{n_l\},n_k,V-k^d]$, in which the volume, $V-k^d$, is formed from the system with volume V by excluding the tiles from a region the size and shape of a length k tile. Because the fraction, $(n_l+1)/V$, of configurations summed in $\Omega_k[\{n_l\},n_k+1,V]$ generate configurations in $\Omega_k[\{n_l,\},n_k,V-k^d]$,

$$\Omega[\{n_l\},n_k+1,V]=\Omega_k[\{n_l\},V-k^d]V/(n_k+1) . \tag{B2}$$

The derivative in Eq. (B1) is equal to

$$\frac{\delta\sigma}{\delta\rho_k}=\ln\left[\frac{\Omega_k[\{n_l\},V-k^d]}{\Omega_1[\{n_l\},V-1]}\frac{n_1}{n_k+1}\right] . \tag{B3}$$

Equation (17) is obtained by expanding the right side of Eq. (B3) and omitting any terms of order $1/V$ or smaller. For a large tile, the dominant effect of the insertion of an additional size k at a specific location is the reduction of the volume available to the rest of the tiles, hence

$$\Omega_k[\{n_l\},V-k^d]\approx\Omega[\{n_l\},V-k^d] .$$

The corrections to this approximation in Eq. (17) are the b_k, which must be of the order of the boundary size, k^{d-1}. In the one-dimensional system, $b_k=0$.

The equilibrium tiling distribution is found by minimizing the free energy as a function of the $\{\rho_k\}$ for $k\geq 2$. Because the concentration of unit length tiles is included only as an explicit function of the other concentrations, no constraint is needed and

$$\beta(\varepsilon_k-k^d\varepsilon_1)=\frac{\delta\sigma}{\delta\rho_k} . \tag{B4}$$

The ε_1 term is required because the inserted length k tile replaces k^d size 1 tiles and

$$e=\frac{E}{V}=\sum_{k\geq 2}\rho_k(\varepsilon_k-k^d\varepsilon_1) . \tag{B5}$$

The substitution of Eq. (15) into Eq. (B4) yields

$$\ln(\rho_k)=-\beta\varepsilon_k-k^d\sigma[\{\rho_l\}]+k^d\sum_{l\geq 2}\rho_l\frac{\delta\sigma}{\delta\rho_l}+O(k^{d-1}) . \tag{B6}$$

The asymptotic behavior of the tile distribution for large k shown in Eq. (11) is proven by using Eqs. (B4) and (B5) to simplify the sum over the entropy derivatives in Eq. (B6).

[1]C. A. Angell, in *Relaxation in Complex Systems*, Proceedings of the Workshop on Relaxations, Blacksburg, 1983, edited by K. Ngai and G. B. Smith (U.S. Dept. of Commerce, Washington, D.C., 1985), p. 3.

[2]C. A. Angell, J. Non-Cryst. Solids **73**, 1 (1985).

[3]F. Spaepen, Mater. Sci. Eng. **97**, 403 (1988).

[4]N. A. Walker, D. M. Lamb, S. T. Adamy, J. Jonas, M. P. Dare-Edwards, J. Phys. Chem. **92**, 3675 (1988).

[5]F. H. Stillinger, J. Chem. Phys. **89**, 6461 (1988).

[6]G. H. Fredrickson, Annu. Rev. Phys. Chem. **39**, 149 (1988).

[7]C. A. Angell, J. Phys. Chem. Solids **49**, 863 (1988).

[8]W. Kauzmann, Chem. Rev. **43**, 219 (1948).

[9]F. H. Stillinger, J. Chem. Phys. **88**, 7818 (1988).

[10]F. H. Stillinger and T. A. Weber, Phys. Rev. A **25**, 978 (1982).

[11]F. H. Stillinger and T. A. Weber, Ann. N.Y. Acad. Sci. **484**, 1 (1986).

[12]T. A. Weber, G. H. Fredrickson, and F. H. Stillinger, Phys. Rev. B **34**, 7461 (1986).

[13]T. A. Weber and F. H. Stillinger, Phys. Rev. B **36**, 7043 (1987).

[14]S. M. Bhattacharjee and E. Helfand, Phys. Rev. A **36**, 3332 (1987).

[15]J. G. Harris and F. H. Stillinger, J. Phys. Chem. **93**, 6893 (1989).

[16]D. R. Nelson, Phys. Rev. B **28**, 5515 (1983).

[17]H. Reiss, Adv. Chem. Phys. **9**, 1 (1965).

[18]T. Hill, *Thermodynamics of Small Systems* (Benjamin, New York, 1963). See also T. Hill, J. Chem. Phys. **36**, 153 (1962).

[19]Y. Imry, Phys. Rev. B **21**, 2042 (1980).

[20]V. Privman and M. E. Fisher, J. Stat. Phys. **33**, 385 (1983).

[21]L. K. Runnels, in *Phase Transitions and Critical Phenomena*, edited by C. Domb and M. S. Green (Academic, New York, 1972), Vol. 2.

[22]A. Bellemans and R. K. Nigram, J. Chem. Phys. **46**, 2922 (1967).

[23]R. M. Nisbet and I. E. Farquhar, Physica **73**, 351 (1974).

[24]F. H. Ree and D. A. Chesnut, Phys. Rev. Lett. **18**, 5 (1967).

[25]W. Kinzel and M. Schick, Phys. Rev. B **24**, 324 (1981).

[26]J. Amar, K. Kaski, and J. D. Gunton, Phys. Rev. B **29**, 1462 (1984).

[27]J. C. Phillips, J. Non-Cryst. Solids **34**, 153 (1979).

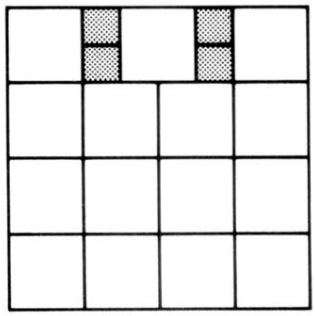

(a)

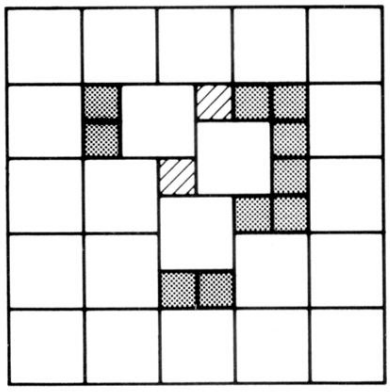

(b)

FIG. 1. Allowed arrangements of 1×1 tiles in a matrix of 2×2 tiles. (a) Dimerized 1×1 tiles. (b) The configuration with the fewest number of 1×1 tiles in which some 1×1 are not dimerized. The hatched squares cannot move relative to each other.